AIAA 95-0530

Vortex Wakes of Rotorcraft

W.J. McCroskey
US Army Aeroflightdynamics Directorate (ATCOM)
NASA Ames Research Center
Moffett Field, CA

33rd Aerospace Sciences Meeting and Exhibit
January 9-12, 1995 / Reno, NV

AIAA 95-0530

VORTEX WAKES OF ROTORCRAFT

W.J. McCroskey*

US Army Aeroflightdynamics Directorate (ATCOM)
NASA Ames Research Center, Moffett Field, CA 94035

Abstract

This paper presents an overview of the complex unsteady vortical flows that comprise the wakes of rotary-wing aircraft; of the effects these tangled vortical structures have on the performance, noise, and vibration; and of some of the recent attempts to measure, predict, and control the phenomena. The main points are illustrated with a number of examples from the recent literature and technical conferences.

Introduction

Rotary-wing aircraft create unsteady vortical flows that tend to be more complex than those of most flight vehicles, even though the fundamental fluid physics may not be significantly different. Figure 1 indicates some peculiar nonlinear aerodynamic phenomena that tend to cause difficulties such as noise, vibrations, and performance limitations of rotorcraft. Many of these phenomena have been the subject of fundamental and applied research for many years, but they remain poorly understood and unpredictable to satisfactory levels of accuracy for engineering purposes. This paper attempts to illustrate some of these flows, to point out the differences with typical fixed-wing applications, and to highlight a number of examples of recent helicopter-related research activities that have focused on these unsteady vortex-dominated flows.

Most of the aerodynamic problems sketched in Fig. 1 arise from some aspect of the tangled vortex wake system that is laid down by the main and tail rotor blades as they rotate and translate through the air. Typical conventional helicopter and tiltrotor wake structures are indicated in Fig. 2 and Fig. 3, From Refs. 1 and 2, respectively. For either configuration, the shed vorticity from the rotor blades tends initially to roll up into discrete, concentrated tip vortices that remain approximately in the cycloidal trace of the blade tips. These concentrated vortices induce local variations in the airflow approaching the rotating blades and the nonrotating components of the rotorcraft. (This rotary-wing counterpart of fixed-wing "downwash" is normally called "inflow.") These vortices also interact with themselves and with other components of the vehicle before evolving into a downstream wake system that, in the mean, superficially resembles the wake of a fixed-wing aircraft. However, its instantaneous, detailed structure remains quite different.

Various aspects of these rotor wakes comprise the basis for most of this paper. Particular emphasis is given to close encounters between wake vortices and rotor blades, referred to as "blade/vortex interactions" (BVI). It should be noted that dynamic stall on the retreating blade of a helicopter rotor is also dominated by unsteady vortical structures; *e.g.*, Fig. 4 [3,4]. This important problem has received considerable attention over the past three decades, but it is too vast a topic to be included here. Finally, brief attention is given at the onset to some of the specialized experimental and theoretical techniques that are used to study rotor wakes. This paper is not intended to be a comprehensive review, but perhaps the limited representative examples, references, and sketchy explanations will guide the interested reader to some valuable information. The

* Senior Research Scientist, Fellow AIAA

majority of the references herein come from the six recent conferences listed below in Table 1. An excellent overview of the status of rotorcraft aerodynamics *circa* 1990, including rotor wakes, can also be found in Ref. 5.

Table 1. Important recent conferences on rotorcraft aeromechanics

49th Annual Forum of the American Helicopter Society, St. Louis, Missouri, 19- 21 May 1993.
19th European Rotorcraft Forum, Cernobbio, Italy, 14-16 September 1993
American Helicopter Society Aeromechanics Specialists' Conference, San Francisco, California, 19-21 January 1994
50th Annual Forum of the American Helicopter Society, Washington, DC, 11- 13 May 1994.
20th European Rotorcraft Forum, Amsterdam, Netherlands, 4-7 September 1994
AGARD Fluid Dynamics Panel Symposium on "Aerodynamics and Aeroacoustics of Rotorcraft, Berlin, Germany, 10-14 October 1994

Experimental Techniques

Flow field diagnostics and measuring techniques are essential for studying wake structures such as those illustrated in Figs. 2 and 3. Flow visualization by means of smoke, water vapor, light-weight particles, neutrally-bouyant helium-filled soap bubbles, and optical techniques, *e.g.*, shadowgraphy, Schlieren, or interferometry, have been used to provide valuable qualitative insights, as well as locating the vortex elements quantitatively. Figure 5 illustrates two alternative visualizations of the tip vortices of a rotor in hovering flight. The vortices in Fig. 5a [6] are made visible by condensation of atmospheric water vapor in the low-pressure core of the vortex; smoke or other tracer particles emitted from the blade tips would produce the same "rotating-frame" visualization. Figure 5b [7] represents the alternative "inertial-frame" visualization; here smoke filaments are introduced in the nonrotating environment and are entrained around the core of the tip vortices. The filaments also show sharp kinks where they are intersected by the vortex sheet that trails from the trailing edges of the blades. It will be important in subsequent figures and discussions to keep in mind these distinctions between the two types of visualizations.

Pitot-static and hot-wire probes have been used to measure rotor wakes, but these have generally been replaced by optical velocimetry. References 8 and 9 contain impressive European examples of 3-D Laser Doppler Velocimetry and Particle Image Velocimetry (PIV), respectively, applied to helicopter Blade/Vortex Interaction (BVI). Also, Lorber, et al [10] recently described the use of PIV in BVI studies, as well as numerous other advanced experimental techniques that are used to study rotorcraft aerodynamics.

Theoretical and Numerical Methods

Wake Vortex Methods. The vortical structures depicted in Figs. 2, 3, and 5 suggest that incompressible vortex-element and vortex-lattice methods should be well suited to analyzing the flow fields induced by rotor wakes. A large body of literature on such applications exists, with much of the activity within the last decade focusing on nonlinear vortex-lattice methods that are classified as "free-wake." This means that each discrete

vortex element, usually tracked in a Lagrangian framework, is allowed to influence the trajectory of all others, and the wake system deforms accordingly. This contrasts with simpler (and computationally less intense) "undistorted" wake models, in which vortex elements or sheets are placed along the trace of the blade tip paths in space, or "prescribed" wake models that use empirical information to define the locations of vortex elements. In either case, the wake-induced inflow at the rotor disc is computed by a Biot-Savart integration.

The accuracy of this general approach and the appropriateness of any particular wake model are highly dependent upon the proximity of the vortex elements to the body or region in question. For example, in hover (Fig. 5), the lift distribution and induced drag of the rotor blades depend crucially on the exact positions of the tip vortices during their early life. Similarly, vibrations and noise are very sensitive to the details of BVI interactions, including "miss distance" and vortex-core structure. Conversely, in level forward flight at moderate cruise speeds, the wake tends to be quickly swept away from the rotor, and the blade airloads are often insensitive to the wake model used.

Representative examples of wakes computed with vortex-lattice and constant-vorticity-contour methods are illustrated in Fig. 6, from Torak and Berezin [11], who analyzed and compared three popular techniques [12-14]. The three predictions are qualitatively similar, and with some notable exceptions, lead to acceptable predictions of lift forces on the blades. Unfortunately, the chordwise forces and pitching moments on the blades, which are much more difficult to predict, were not reported in Ref. 11.

Nonlinear aerodynamic effects in the immediate vicinity of the blades, such as shock waves, viscous/inviscid interaction, or stall, have often been treated by adding empirical corrections or other modifications to linear lifting-line or lifting-surface models. For example, Ref. 15 uses a second-order lifting line theory and experimentally-derived two-dimensional airfoil data, corrected for dynamic stall, blade sweep, tip losses, and unsteady blade motion.

Hybrid Coupling of Vortex Wakes with CFD Codes. Within the past decade, many investigators have coupled computational fluid dynamics (CFD) codes for the nonlinear "near field" with various vortex methods for the wakes, or "far field." One common iterative method of implementing this hybrid coupling, pioneered by Tung, *et al* [16] is illustrated in Fig. 7. The inflow and outflow boundary conditions on a CFD domain, of limited extent, come from the wake model; and the airloads that determine the near-field trailing vorticity, which is required to initiate the wake calculation, are computed by the CFD code. The wake-vortex elements within the CFD domain can be introduced by any of several models, such as those illustrated in Fig. 8 from Ref. 6. The circulation coupling applied through branch cuts is suitable for potential methods, whereas the velocity coupling is more general. However, it requires calculating the velocity induced by the vortex elements, via the Biot-Savart law, throughout the flow field. The implementation of the α-coupling is normally done by "transpiration" boundary conditions on the surface of the blade, and therefore is simpler and less-computationally intensive. Reference 6 gives a more detailed summary of these coupling methods.

An alternative treatment of the vortical wake that couples particularly well with either incompressible or compressible potential flow CFD codes has been pioneered by Steinhoff and his colleagues, called the "vorticity embedding" method [17]. Illustrated in Fig. 9 from Ref. 6, vorticity embedding is a variation on the velocity coupling method described above, wherein the velocity field is represented by $\boldsymbol{V} = \boldsymbol{\Omega} \times \boldsymbol{r} + \boldsymbol{Q}^{\boldsymbol{v}} + \nabla \phi$ (in hover). The details are given in Refs. 6 and 17; briefly, the circulation representing the shed wake is satisfied by a somewhat contrived velocity field, Q^v, whose curl defines a vorticity *distribution* within a wake sheet. The thickness of the sheet is finite, although small compared to other dimensions of the problem, and its path is traced by means of Lagrangian markers. However, this Q^v can actually be chosen to produce the correct induced velocities outside the sheet, to be non-zero only within the sheet, and to have its nonphysical properties canceled by the particular solution, $\nabla \phi$, to the continuity

equation. The end result is that Q^v only has to be computed in a limited domain, thereby overcoming the objections to the usual velocity-coupling method described in the preceding paragraph.

CFD Methods for Wakes. This approach attempts to bypass the tip-vortex formation and core-modeling issues of the vortex methods and the coupling issues of the hybrid schemes by directly simulating the entire flow field with a unified differential method, *i.e.,* Computational Fluid Dynamics. This was first accomplished using an Euler code by Kroll [18], followed by numerous investigators in the US, Europe, and Asia (13 papers presented in the conferences listed in Table 1, for example). Reference 6 summarizes the progress made in the late 1980's, and Landgrebe [19] recently outlined the primary Euler and Navier-Stokes investigations in the US.

Since the summary paper by the author in 1988 [20], calculation of transonic effects on advancing blade tips of complex geometry has almost become routine, and an impressive solution for a nearly-complete tiltrotor aircraft has been published [21]. Also, the frustrations noted in Ref. 20 in calculating *accurately* the details of tip-vortex formation, illustrated in Fig. 10 from Ref. 22, with Navier-Stokes codes have been largely overcome [23], although the computations are still too expensive for routine applications. Figure 11 shows the measured and computed pressure distributions on the tip beneath the vortex [23]. The good agreement around $x/c = 0.9$, which was not attained in previous investigations, is a key indicator of success for this problem.

However, progress in calculating the detailed vortex structures in rotor wakes has been less satisfactory. In particular, the numerical diffusion inherent in finite-difference or finite-volume codes spreads the vorticity and reduces the peak velocities in the core of the tip vortex unnaturally as it rolls up and convects into the wake. This significantly degrades the detailed predictions of blade/vortex interactions, for example. However, total circulation associated with the vortex remains approximately constant, so that the mean inflow tends to be approximately correct, allowing reasonable predictions of the blade airloads in some cases [24-26]. This is illustrated in Figs. 12 and 13 from Ref. 26. Although smeared, the wake shows a qualitatively-correct geometry, and the lift on the blades is approximately correct after three rotor revolutions.

The problem of numerical diffusion in the wake is exacerbated by the limits to the numbers of fixed grid points that can be realistically employed, leading logically to solution-adaptive or multi-block grids in the wake. Strawn and Barth [27] pioneered the application of adaptive grid refinement of unstructured grids to improve the resolution of Euler calculations in rotor wakes, as illustrated in Fig. 14. To obtain a better Navier-Stokes resolution of the flow field, Ahmad and Duque [26] used an embedded multi-block system of structured grids attached to the rotating and flapping blades, moving through a stationary background grid that roughly captured the wake structure (Figs 12 and 13). This methodology is essentially the same as that of Ref. 21, with the addition of prescribed flapping and lead-lag motion of the blades. In all, about 1.6 million grid points were used. Future plans are to replace the grids in the wake grids with solution- unstructured grids, following the general plan of Ref. 28, shown in Fig. 15.

Finally, Steinhoff, et al [29] presented a new method that introduces an auxiliary scalar field to counteract the effect of numerical diffusion in standard CFD codes, within the thin, concentrated vortical region representing the rotor wake. The extra "vorticity confinement" term is added locally to the momentum equations on a fixed, Eulerian grid, it is non-zero only within the vortical regions, and it does not change the total vorticity or mass within those regions. In principle, the confinement term permits vortical structures to be convected without diffusion, but it can be switched off in viscous-dominated regions such as boundary layers on solid bodies. Preliminary results given in Refs. 29 and 30 indicate that this method should be promising for rotor wake calculations and BVI.

Hover and Related Problems

Isolated Rotors in Free Air. Figure 5 illustrates many of the basic physical features of

the wakes of rotorcraft hovering out of ground effect. References 25, 31, and 32 provide detailed evaluations of some of the more sophisticated theoretical and numerical prediction techniques currently available. The vortex-embedding code HELIX-I has emerged as a good all-around compromise between accuracy, generality (*i.e.*, the ability to treat complex or non-standard blade shapes), and computational efficiency.

Hover in Ground Effect. Figure 16 from Ref. [33] illustrates the additional complexities that arise when a helicopter operates near the ground. Reference 34 is representative of the ability to model the interaction of the main rotor with a solid boundary nearby, and the recent experimental investigation of Light [35] is noteworthy.

Vertical Flight and the Vortex Ring State. Vertical climb represents a relatively benign environment for the main rotor(s) of a helicopter, as the wake moves more rapidly away from the blades than in hover. However, the inverse situation, descending into the wake at rates on the order of half the average inflow velocity in hover, produces an irregular flow field and higher power required for equilibrium [36]. This is illustrated in Fig. 17 from Ref. [36]. Detailed measurements were reported recently by Xin and Gao [37], but predictions of this phenomenon remain elusive.

Level Forward Flight - Moderate to High Speeds

As shown in Figs. 2 and 3, the wake of rotorcraft in forward flight is swept downstream, more so as the "advance ratio," μ (the ratio of flight speed, V_∞, to blade tip speed, ΩR), increases. However, there are multiple possibilities for helicopter blades to encounter, or at least pass above, the tip vortices shed by preceding blades. Furthermore, the equilibrium balance, or "trim," of a rotor dictates reducing the blade-element angles of attack on the "advancing" blade, where the rotational and translational velocities add together, and increasing the angles on the "retreating" blade, where they subtract. These factors produce three important aerodynamic complications. First, transonic conditions can arise near the tips of the advancing blades. Second, stall conditions can arise on the retreating blade, and the transitory nature of this stall can be very different from fixed-wing quasi-static stall. In extreme cases, deep dynamic stall on the retreating blade is dominated by a different type of vortical structure, the dynamic stall vortex depicted in Fig. 4.

Finally, the aerodynamic loading and the associated spanwise circulation distribution on the blades vary periodically, producing a complicated mixture of spanwise vortical structures shed from the trailing edge and tip vortices forming with varying strength. This is depicted in Fig. 18, which indicates that even the sign of the circulation of the trailing vortices may change. The actual structure of such a vortical flow is not well understood, nor predicted satisfactorily up to now.

Assessing the accuracy of predictions of the airloads on rotor blades in forward flight is difficult, complicated, and challenging. A recent Navier-Stokes CFD solution for a relatively benign case, Figs. 12 and 13 was discussed earlier. References 11, 38-40 are a few among many in the literature that attempt to address the accuracy issues for the methods more commonly used today. Generally, it can be said that the spanwise lift distribution can be predicted reasonably well, except when blade/vortex interactions are important. Pitching moments or chordwise forces are seldom predicted satisfactorily.

Aerodynamic Interference

Figures 1-3 suggest some of the wide range of aerodynamic-interference problems that can exist on rotorcraft. Several specific examples are discussed briefly in this section.

Main/Tail Rotor Interference. Tail rotors are used on helicopters with a single main rotor to balance the torque of the main rotor and for directional control in hover and low speed flight. Their thrust, power required, vibratory loads, and noise can be adversely affected if they ingest the vortex wake of the main rotor. A number of investigators [41-46] have studied this problem recently, experimentally and computationally. Figure 19, derived from an earlier experimental study [47], shows the

additional complications that arise near the ground in a strong crosswind. The time-averaged main rotor wake rolls up into a horseshoe vortex just above the ground that extends downwind. Severe control and vibration problems arise when the yaw angle of the helicopter results in one leg of the horseshoe vortex passing through the tail rotor.

Tandem and Co-Axial Rotors. Some helicopters employ two main rotors, in either tandem or co-axial configurations. Figure 20 from Ref. 48 shows the tip vortex trajectories computed with an advanced lifting-surface and vortex-filament method. Baron and Boffadossi [43] also analyzed tandem rotors with a vortex-lattice method. A comprehensive review of co-axial rotors by Coleman [49] and a recent paper by Akimov [50] describing Russian co-axial rotors are noteworthy. Favorable interference between the rotors, combined with the absence of additional power required to drive a tail rotor, can lead to performance benefits in hover for this configuration.

Helicopter Rotor/Body Interference. Most of the interactional aerodynamics methodology developed up to now has used panel codes for the fuselage and vortex-lattice methods for the rotor wake. Several examples are reviewed in Ref. 51, and the more recent Refs. 52-57 are among many may be mentioned. The Navier-Stokes work of Zori, et al [58] is noteworthy for cases where time-averaged results suffice. Studies of the interactions between the main rotor and the empannage of a helicopter have been reported on recently in Refs. 10, 59, and 60.

Tiltrotor Rotor/Body Interference. As shown in Fig. 3, rotor blade vortices interact with the airframe for this class of aircraft, as well. However, there are some special problems, as well. Figure 3a indicates schematically the complex flow that is produced when the downwash of the rotors impinges on the wing of a typical tiltrotor aircraft. The "fountain" that is produced when the wakes from the two sides of the vehicle meet tends to be re-ingested into the rotors, producing additional noise and vibrations from this unsteadiness [2]. In addition, the downward impingement produces a downward force on the wing that is typically on the order of 10% of the overall rotor thrust, thereby reducing the hovering efficiency of the aircraft.

These hover-download and fountain effects have been the object of numerous investigations over many years. Figure 21 shows the results of a recent time-accurate Navier-Stokes CFD simulation, using moving multi-block structured grid strategies, to be published in Ref. 61. The figure shows the flow produced by a rotor, wing, and nacelle combination, after the rotor has completed 13 revolutions starting from rest. Detailed comparisons with the experiment of Felker, et al [62] are underway.

Figure 22 from Ref. 21 shows the results of a similar CFD simulation of the V-22 aircraft in transitional flight. The flowfield details and unsteady pressure distributions presented in Ref. 21 provide insight into the unsteady airloads produced on the airframe from the periodic passage of the rotor blades and their associated wakes.

Blade / Vortex Interactions

The Basic Physics. The aerodynamic interaction between rotor blades and the vortical wakes that they create is an important source of vibrations and external noise, and this problem is perhaps the number one challenge in rotorcraft aerodynamics today. Accordingly, BVI has been the subject of extensive analytical, computational, and experimental studies, which are far too numerous to list here. The basic problem, which is most acute in descending flight or maneuvers at moderate advance ratios, is illustrated in Figs. 23-25. Figure 23 suggests that many close encounters are possible; however, the most impulsive ones are those in which the blade cuts through a vortex at a shallow angle with respect to the leading edge; *i.e.*, Fig 23b. Figure 24 from Heller, et al [63] is an example of the time history of pressure transducers near the leading edge during one blade revolution in BVI conditions, and Fig. 25 shows the associated acoustic signatures and spectral responses of microphones beneath the rotor [63]. For these operating conditions, impulsive noise in the form of sharp pressure spikes is generated from BVI interactions on both the advancing and retreating sides of the rotor disc. Often the advancing-side BVI noise

is the greater problem in terminal-area flight operations such as landing approaches, but both must be considered. In fact, BVI on the retreating blade can also lead to retreating-blade stall under heavily loaded conditions.

The primary nondimensional parameters that appear to govern the severity of this complex phenomenon are the strength of the vortex, the separation distance between the vortex and the blade during the encounter, and the angle between the axis of the vortex and the leading-edge of the blade (Λ in Fig. 23). Parameters that are arguably secondary, but still important, include the detailed structure of the vortex core, the shape of the leading edge of the blade, the lift on the blade just prior to the encounter, the Mach number of the local flow approaching the blade during the encounter, and possibly the Reynolds number.

Two Focused Approaches. Attempts to model, predict, and/or control or reduce BVI-induced noise and vibrations by practical means have encountered multiple difficulties. The blade position in space and the position and structure of the vortical wake cannot be predicted with the precision required to determine the unsteady blade pressures reliably, and hence the predicted acoustic radiation is usually inaccurate. Experimentalist face the daunting challenge of measuring the instantaneous blade position, the rotating blade-pressure loadings, the exact positions and structure of the unsteady wake vortices, and the acoustic field simultaneously.

Two important, related research approaches have evolved to meet this challenge. The first is to try to isolate the fundamentals; for example, the quasi-two-dimensional representation depicted in Fig. 23b. Numerous analytical and computational studies have led to reasonable predictions of isolated airfoil/vortex interactions, although this strictly 2-D model problem is extremely difficult to replicate experimentally with sufficient information and precision to validate the predictions completely. A large number of investigations, of which Refs. 64-67 are but a few representative examples, have established most of the fundamental behavior in the idealized two-dimensional case.

However, special-purpose rotor experiments have been conceived and conducted [9, 68-69] that remove some of the difficulties in determining the structure of the incident vortex while retaining the essence of the aerodynamic interaction itself. As indicated schematically in Fig. 26, a controlled vortex is created upstream of an otherwise nonlifting rotor blade that is highly instrumented. The miss distance and relative sweep angle Λ are controlled by the position of the upstream wing tip, and the strength of the vortex is controlled by the incidence of the wing. The data generated by these experiments is beginning to be used by the research community, and will likely continue to do so.

The second approach is to pool international experimental resources and to attempt to measure and document as much of the blade motion, blade surface pressures, flow field, and acoustic field as possible under realistic rotor conditions. The first such collaborative effort, involving six research institutes in four countries is the Higher-Harmonic Control Acoustic Rotor Test project (HART), which was recently reported on by Yu, et al [70] and Kube, et al [8]. The test setup in the Duits-Nederlandse Windtunnel (DNW) in the Netherlands is shown in Fig. 27. A 4-meter dia. model rotor, geometrically and aeroelastically scaled from the BO-105 helicopter, was tested in the 6m x 8m open-jet anechoic test section of the DNW under BVI conditions, with and without higher-harmonic blade pitch control inputs that reduce BVI noise and/or vibrations. The extensive data were still being reduced and analyzed at the time of the writing of this paper, but Fig. 28 from Ref. 70 illustrates the value of having many different simultaneous measurements. The hypothetical plan view on the right side of the figure indicates that many blade/vortex encounters are possible, but the optical flow-field and blade-deflection measurements revealed that "vortex 5" is the one responsible for the BVI noise and vibrations in this particular case.

The HART project also includes a coordinated effort by each participant to predict the aerodynamic and acoustic results of the test, with and without higher-harmonic control (HHC) [70,71]. The combined experimental and analytical efforts of the HART project will help

the entire rotorcraft community understand and predict BVI better as the results of the investigations are disseminated at future technical conferences.

Control or Reduction of BVI. Of the many schemes that have been proposed for reducing BVI noise and vibrations, most attempt to modify either the strength of the tip vortices or their position relative to the blades. These concepts are illustrated Fig. 29 from Ref. 72. Brooks [73] recently reviewed a number of "passive" blade modifications that have been tried over the years to alleviate BVI effects by modifying the initial formation and rollup of the tip vortices, *e.g.*, Figs. 30 and 31, and two new proposals, Fig. 32. Most modern helicopters employ some sort of swept tip, but no single tip shape has emerged as producing the desired BVI results over a range of operating conditions.

Alternatively, a number of "active" schemes have been proposed to alter the tip vortices and/or the miss distances by changing the pitch or flapping of the rotor blades appropriately. These include active control of a trailing-edge flap, higher-harmonic pitch inputs to the rotor control system using actuators in the nonrotating system under the rotor swashplate (HHC), and arbitrary inputs to control actuators that replace the blade pitch links in the rotating system (Individual Blade Control, IBC). A recent model rotor experiment with an open-loop trailing-edge flap [74] showed that the acoustic spectrum was altered, and that the BVI noise could be reduced or increased, when the flap was deflected with a variety of prescribed schedules. An important objective of the HART program discussed above is to explore the previously observed HHC results of Kube, et al [75]; namely, that HHC generally produced higher vibrations when the BVI noise was reduced, and vice versa. The desired result, of course, is to reduce both simultaneously. Finally, the recent IBC experiment of Niesl, et al [76] showed that the additional freedom afforded by the pitch actuators in the rotating system enabled significant noise and vibration reduction to be achieved simultaneously.

Concluding Remarks.

The examples taken from the recent literature on the wakes of helicopters show the complexity of this class of vortical flows; but they also indicate the considerable progress that has been made over the past decade toward understanding, describing, and predicting wake effects on practical aspects of modern rotorcraft. The recent advances in experimental techniques, the new numerical methods being developed, the recently-acquired comprehensive data bases, and the ideas being explored for BVI alleviation can be expected reap significant benefits to the rotorcraft community over the next decade.

Acknowledgements

The invaluable contributors to this paper are the many investigators whose ideas and results are cited in the text. In addition, the author gratefully acknowledges the assistance of a number of individuals who kindly shared their creative results and information by means of personal communications, and/or helped prepare the figures and accompanying video. These include W.G. Bousman, J.O. Bridgeman, T.F. Brooks, F.X. Caradonna, J.S. Dacles-Mariani, L.U. Dadone, E.P.N. Duque, C.N. Gong, A.A. Hassan, H. Heller, A.J. Landgrebe, J.G. Leishman, R.L. Meakin, U.B. Mehta, R.A. Ormiston, Marianne Rudolph, K.A. Sava, D.B. Signor, R.C. Strawn, A.A. Swanson, and Y.H. Yu.

References

1. *Aviatsiya i Kosmonautika,* 1973.

2. McVeigh, M.A., Greuer, W.K., and Paisley, D.J., "Rotor/Airframe Interactions on Tiltrotor Aircraft," Proc. 44th American Helicopter Society Annual Forum, Washington, DC, June 1988.

3. Mehta, U.B., "Dynamic Stall of an Oscillating Airfoil," Paper No. 23, AGARD Conference Proceedings 227 on Unsteady Aerodynamics, 1977.

4. Werlé, H, "Flow Visualization Techniques for the Study of High Incidence Aerodynamics," Paper No. 3, AGARD Lecture Series No. 121 on High Angle-of-Attack Aerodynamics, 1982.

5. Aerodynamics of Rotorcraft, AGARD Report No. 781, 1990.

6. Caradonna, F.X., "The Application of CFD to Rotary Wing Flow Problems," Paper No. 5, Aerodynamics of Rotorcraft, AGARD Report No. 781, 1990.

7. Landgrebe, A.J., "The Wake Geometry of a Hovering Helicopter Rotor and Its Influence on Rotor Performance," *J. American Helicopter Soc.*, Vol. 17, No. 4, pp. 3-15, Oct. 1972.

8. Kube, R., Splettstoesser, Wagner, W., Seelhorst, U., Yu, Y.H., Boutier, A., Micheli, F., and Mercker, E., "Initial Results form the Higher Harmonic Control Aeroacoustic Rotor Test (HART) in the German-Dutch Wind Tunnel," Paper No. 25, Proc. AGARD Conference on Aerodynamics and Aeroacoustics of Rotorcraft, Berlin, GE, 1994.

9. Coton, F.N., de la Iglesia Moreno, F., McDonald Galbraith, R.A., and Horner, M.B., "A Three-Dimensional Model of Low Speed Blade-Vortex Interaction," Proc. 20th European Rotorcraft Forum, Amsterdam, NE, 1994.

10. Lorber, P.F., Stauter, R.C., Haas, R.J., Anderson, T.J., Torok, M.S., and Kohlhepp, F.W., "Techniques for Comprehensive Measurement of Model Helicopter Aerodynamics," Proc. 50th American Helicopter Society Annual Forum, Washington, DC, May, 1994.

11. Torok, M.S., and Berezin, C.R., "Aerodynamic and Wake Methodology Evaluation Using Model UH-60A Experimental Data," *J. American Helicopter Soc.*, Vol. 39, No. 2, pp. 21-29, Apr. 1994.

12. Egolf, T.A., "Helicopter Free Wake Prediction of Complex Wake Structures Under Blade-Vortex Interaction Operating Conditions," Proc. 44th American Helicopter Society Annual Forum, Washington, DC, June 1988.

13. Johnson, W.R., "Wake Model for Helicopter Rotors in High Speed Flight," NASA CR 177507, Nov. 1988.

14. Quackenbush, T., Wachspress, D., and Boschitsch, A., "Computation of Rotor Aerodynamic Loads with a Constant Vorticity Contour Free Wake Model," AIAA Applied Aerodynamics Conference, Baltimore, MD, 1991.

15. Johnson, W.R., "CAMRAD/JA; A Comprehensive Analytical Model of Rotorcraft Aerodynamics; Johnson Aeronautics Version," Johnson Aeronautics, Palo Alto, CA. 1988.

16. Tung, C., Caradonna, F.X., and Johnson, W., "The Prediction of Transonic Flows on Advancing Rotors," *J. American Helicopter Soc.*, Vol. 31, No. 3, pp. 4-9, July 1986.

17. Steinhoff, J, and Ramachandran, R., "Free Wake Analysis of Compressible Rotor Flows, *J. AIAA*, Vol. 28, No. 3, pp 426-431, Mar. 1990.

18. Kroll, N., "Computation of the Flow Fields of Propellers and Hovering Rotors Using the Euler Equations," Proc. 12th European Rotorcraft Forum, Garmisch-Partenkirchen, GE, 1986.

19. Landgrebe, A.J., "New Directions in Rotorcraft Computational Aerodynamics Research in the U.S.," Paper No. 1, Proc. AGARD Conference on Aerodynamics and Aeroacoustics of Rotorcraft, Berlin, GE, 1994.

20. McCroskey, W.J., "Some Rotorcraft Application of Computational Fluid Dynamics," Proc. 2nd Internat. Conf. on Basic Rotorcraft Research," College Park, MD, 1988; also NASA TM 100066, Mar. 1988.

21. Meakin, R., "Moving Body Overset Grid Methods for Complete Aircraft Tiltrotor Simulations," AIAA Paper 93-3350, Orlando, FL, 1993.

22. Werlé, H. "Transition et Turbulence," ONERA Note Technique 1987-7, 1987.

23. Dacles-Mariani, J.S., Zilliac, G.G., Chow, J.S., and Bradshaw, P., "A Numerical/ Experimental Study of a Wingtip Vortex in the Near Field," to be published in *AIAA Journal*; 1995; also AIAA Papers 93-3010 and 93-3011, Orlando, FL, 1993.

24. Srinivasan, G.R, Raghavan, V., Duque, E.P.N., and McCroskey, W.J., "Flowfield Analysis of Modern Helicopter Rotors in Hover by Navier-Stokes Method," *J. American*

Helicopter Soc., Vol. 38, No. 3, pp. 3-13, July, 1993.

25. Wake, B.E., and Baeder, J.D., "Evaluation of the TURNS Analysis for Hover Performance Prediction," Paper 3.2, Proc. AHS Aeromechanics Specialists Conf., San Francisco, CA, Jan. 1944.

26. Ahmad, J., and Duque, E.P.N., "Helicopter Rotor Blade Computation in Unsteady Flows Using Moving Embedded Grids," AIAA Paper 94-1922, Colorado Springs, CO, 1994.

27. Strawn, R.C., and Barth, T.J., "A Finite-Volume Euler Solver for Computing Rotary-Wing Aerodynamics on Unstructured Meshes," *J. American Helicopter Soc.*, Vol. 38, No. 2, pp. 3-13, Apr. 1993.

28. Duque, E.P.N., "A Strucutured/Unstructured Embedded Grid Solver for Helicopter Rotor Flows," Proc. 50th American Helicopter Society Annual Forum, Washington, DC, May, 1994.

29. Steinhoff, J, Wenren, Y., Mersch, T., and Senge, H., "Computational Vorticity Capturing: Application to Helicoper Rotor Flow," AIAA Paper 92-0056, Reno, NV, 1992.

30. Wang, C.M., Bridgemen, J.O., Steinhoff, J., and Wenren, Y., "The Application of Computational Vorticity Confinement to Helicopter Rotor and Body Flows," Proc. 49th American Helicopter Society Annual Forum, St. Louis, MO, May, 1993.

31. Tung, C., and Lee, S., "Evaluation of Hover Performance Prediction Codes," Proc. 50th American Helicopter Society Annual Forum, Washington, DC, May, 1994.

32. Ramachandran, K., Owen, S.J., Caradonna, F.X., and Moffitt, R.C. "Hover Performance Prediction Using CFD," Proc. 50th American Helicopter Society Annual Forum, Washington, DC, May, 1994.

33. Prouty, R.W., *More Helicopter Aerodynamics*, PJS Publications, Inc., Peoria, IL, 1988.

34. Baron, A., and Boffadossi, M., "Numerical Simulation of Unsteady Rotor Wakes," Proc. 17th European Rotorcraft Forum, Berlin, GE, 1991.

35. Light, J.S., "Tip Vortex Geometry of a Hovering Helicopter Rotor in Ground Effect," *J. American Helicopter Soc.*, Vol. 38, No. 2, pp. 34-42, Apr. 1993.

36. Prouty, R.W., *Practical Helicopter Aerodynamics*, PJS Publications, Inc., Peoria, IL, 1982.

37. Xin, H., and Gao, Z., "An Experimental Investigation of Model Rotors Operating in Vertical Descent," Proc. 19th European Rotorcraft Forum, Cernobbio, IT, 1993.

38. Young., Bousman, W.G., Maier, T.H., Toulmay, F., and Gilaber, N., "Lifting Line Predictions for a Swept Tip Rotor Blade," Proc. 47th American Helicopter Society Annual Forum, Phoenix, AZ, May, 1991.

39. Strawn, R.C., and Bridgeman, J.O., "An Improved Three-Dimensional Aerodynamics Model for Helicopter Airloads Prediction," AIAA Paper 91-0767, Reno, NV, 1991.

40. Yen, J.G., and Yuce, M., "Correltation of Pitch-Link Loads in Deep Stall on Bearingless Rotors," *J. American Helicopter Soc.*, Vol. 37, No. 4, pp. 4-15, Oct. 1992.

41. Ellin, A.D.S., "An In-flight Investigation of LYNX AH MK5 Main Rotor/Tail Rotor Interactions," Proc. 19th European Rotorcraft Forum, Cernobbio, IT, 1993.

42. Srinivas, V., Chopra, I., Haas, D., and McCool, K., "Prediction of Yaw Control Effectiveness and Tail Rotor Loads," Proc. 19th European Rotorcraft Forum, Cernobbio, IT, 1993.

43. Baron, A., and Boffadossi, M., "Unsteady Free Wake Analysis of Closely Interfering Helicopter Rotors," Proc. 18th European Rotorcraft Forum, Avignon, FR, 1992.

44. Leverton, J.W., and Pike, T.C., "The Importance of Tail Rotor Interaction as an Acoustic Source," Proc. 49th American Helicopter Society Annual Forum, St. Louis, MO, May, 1993.

45. Schultz, K.-J., and Splettstoesser, W.R., "Helicopter Main Rotor/Tail Rotor Noise Radiation Characteristics from Scaled Model Rotor Experiments in the DNW," Proc. 49th American Helicopter Society Annual Forum, St. Louis, MO, May, 1993.

47. Empey, R.W., and Ormiston, R.A., "Tail Rotor Thrust on a 5.5-foot Helicopter Model in Ground Effect," Proc. 30th American Helicopter Society Annual Forum, Washington, DC, May 1974.

48. Leishman, J.G., and Bagai, A., "Free Wake Analysis of Twin-Rotor Systems, Proc. 20th European Rotorcraft Forum, Amsterdam, NE, 1994.

49. Coleman, C.P., "Survey of Theoretical and Experimental Coaxial Rotor Aerodynamic Research," Proc. 19th European Rotorcraft Forum, Cernobbio, IT, 1993.

50. Akimov, A.I., Butov, V.P., Bourtsev, B.N., and Selemenev, S.V., "Flight Investigatin of Coaxial Rotor Tip Vortex Structure," Proc. 30th American Helicopter Society Annual Forum, Washington, DC, May 1974.

51. Ahmed, S.R., "Fuselage Aerodynamics Design Issues and Rotor/Fuselage Interactional Aerodynamics. Part II: Theoretical Methods," Paper No. 4, Aerodynamics of Rotorcraft, AGARD Report No. 781, 1990.

52. Clark, D.R., and Maskew, B., "A Re-Examination of the Aerodynamics of Hovering Rotors including the Presence of the Fuselage," Proc. 47th American Helicopter Society Annual Forum, Phoenix, AZ, May, 1991.

53. Lorber, P.F., and Egolf, T.A., "an Unsteady Helicopter Rotor-Fuselage Interaction Analysis," NASA CR 4178, Sept. 1988.

54. Quackenbush, T.R., Bliss, D.B., Lam, C-M.G, and Katz, A., "New Vortex/Surface Interaction Methods for the Prediction of Wake-Induced Airframe Loads," Proc. 46th American Helicopter Society Annual Forum, Washington, DC, May, 1990.

55. Crouse, G.L., Leishman, J.G., and Bi, N., "Theoretical and Experimental Study of Unsteady Rotor/Body Aerodynamic Interactions," Proc. 46th American Helicopter Society Annual Forum, Washington, DC, May, 1990.

56. Berry, J.D., and Althoff, S.L., "Inflow Velocity Perturbations Due to Fuselage Effects in the Presence of a Fully Interactive Wake," 46th American Helicopter Society Annual Forum, Washington, DC, May, 1990.

57. Gasser, D., Bettschart, N., and Drouin, B., "Theoretical and Experimental Studies on Unsteady Rotor-Fuselage Interactional Aerodynamics," Proc. American Helicopter Society Vertical Lift Aircraft Design Conference, San Francisco, CA, Jan. 1995.

58. Zori, L.A.J., Mathur, S.R., and Rajagopalan, R.G., "Navier-Stokes Calculation of Rotor/Airframe Interaction," Proc. 48th American Helicopter Society Annual Forum, Washington, DC, May, 1992.

59. Torok, M.S., and Ream, D.T., "Investigation of Empennage Airloads Induced by a Helicopter Main Rotor Wake," Proc. 49th American Helicopter Society Annual Forum, St. Louis, MO, May, 1993.

60. Frederickson, K.C., and Lamb, J.R., "Experimental Investigation of Main Rotor Wake Induced Empennage Vibratory Airloads for the RAH-66 Comanche Helicopter," Proc. 49th American Helicopter Society Annual Forum, St. Louis, MO, May, 1993.

61. Meakin, R.L., "Unsteady Simulation of the Viscous Flow about a V-22 Rotor and Wing in Hover," Submitted to AIAA Atmospheric Flight Mechanics Conf., Baltimore, MD, Aug. 1995.

62. Felker, F., Shinoda, P., Heffernan, and Sheehy, F., "Wing Force and Surface Pressure Data from a Hover Test of a 0.658 Scale V-22 Rotor and Wing," NASA TM 102244, Feb. 1990.

63. Heller, H., Schultz, K-J., Ahmed, S.R., and Splettstoesser, W., "Unsteady Surface Pressure Characteristics on Helicopter Blades: A key to the Physics of Rotor Noise," 19th ICAS-Congress Paper ICAS 94-2.7.2, Aneheim, CA, Sept. 1994.

64. Srinivasan, G.R., and McCroskey, W.J., "Numerical Simulations of Unsteady Airfoil-Vortex Interactions," *Vertica,* Vol. 11, No. 1-2, pp. 3-28, Jan. 1987.

65. Baeder, J.D., "Computation of Non-Linear Acoustics in Two-Dimensional Blade-Vortex Interactions," Proc. 13th European Rotorcraft Forum, Arles, FR, 1987.

66. Ehrenfried, K., Meier, G.E.A., and Obermeier, F., "Sound Produced by Vortex-Airfoil Interaction," Proc. 17th European Rotorcraft Forum, Berlin, GE, 1991.

67. Xue, Y., and Lyrintzis, A.S., "Transonic Blade-Vortex Interactions: Noise Reduction," *J Aircraft*, Vol. 30, N0. 3, pp. 408-410, May-June 1993.

68. Caradonna, F.X., Lautenschlager, J.L., and Silva, M.J., "An Experimental Study of Rotor-Vortex Interactions," AIAA Paper 88-0045, Reno, NV, Jan. 1988.

69. Kitaplioglu, C., and Caraconna, F.X., "A Study of Blade-Vortex Aeroacoustics Utilizing an Independently Generated Vortex," Paper No. 20, Proc. AGARD Conference on Aerodynamics and Aeroacoustics of Rotorcraft, Berlin, GE, 1994.

70. Yu, Y.H., Gmelin, B., Heller, H., Philippe, J.J., Mercker, E., and Preisser, J.S., "HCC Aeroacoustics Rotor Test at the DNW - The Joint German/French/US HART Project," Proc. 20th European Rotorcraft Forum, Amsterdam, NE, 1994.

71. Beaumier, P., Prieur, J., Rahier, G., Demargne, A., Tung, C., Gallman, J.M., Yu, Y.H., Kube, R., Van der Wall, B.G., Schultz, K.J., Splettstoesser, W.R., Brooks, T.F., Burley, C.L., Boyd, D.D., Jr., "Effect of Higher Harmonic Control on Helicopter Rotor Blade-Vortex Interaction Noise: Prediction and Initial Validation," Paper No. 26, Proc. AGARD Conference on Aerodynamics and Aeroacoustics of Rotorcraft, Berlin, GE, 1994.

72. Brooks, T.F., and Booth, E.R., Jr., "The Effects of Higher Harmonic Control on Blade-Vortex Interaction Noise and Vibrations," *J. American Helicopter Soc.,* Vol. 38, No. 3, pp. 45-55, July. 1993.

73. Brooks, T.F., "Studies of Blade-Vortex Interaction Noise Reduction by Rotor Blade Modification," Proc. 1993 National Conference on Noise Control, pp. 57-66, Williamsburg, VA, May 1993.

74. Marcolini, M.A., Booth, E.R., Jr., Tadghighi, H., Hassan, A.A., , Smith, C.D., and Becker, L.E., "Control of BVI Noise Using an Active Trailing Edge Flap," Proc. American Helicopter Society Vertical Lift Aircraft Design Conference, San Francisco, CA, Jan. 1995.

75. Kube, R., Achache, M., Niesl, G., and Splettstoesser, W.R., "A Closed Loop Controller for BVI Impulsive Noise Reduction by Higher Harmonic Control," Proc. 48th American Helicopter Society Annual Forum, Washington, DC, May, 1992.

76. Niesl, G., Swanson, S.M., Jacklin, S.A., Blaas, A., and Kube, R., "Effect of Individual Blade Control on Noise Radiation," Paper No. 19, Proc. AGARD Conference on Aerodynamics and Aeroacoustics of Rotorcraft, Berlin, GE, 1994.

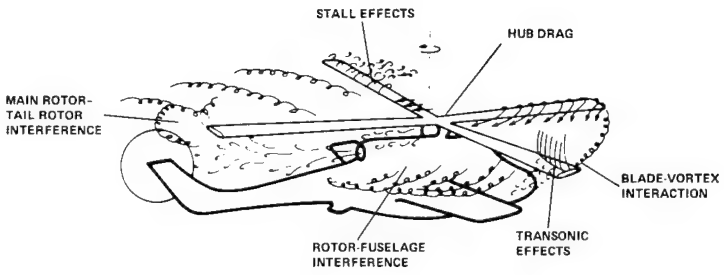

Fig. 1 Complexities of helicopter aerodynamics.

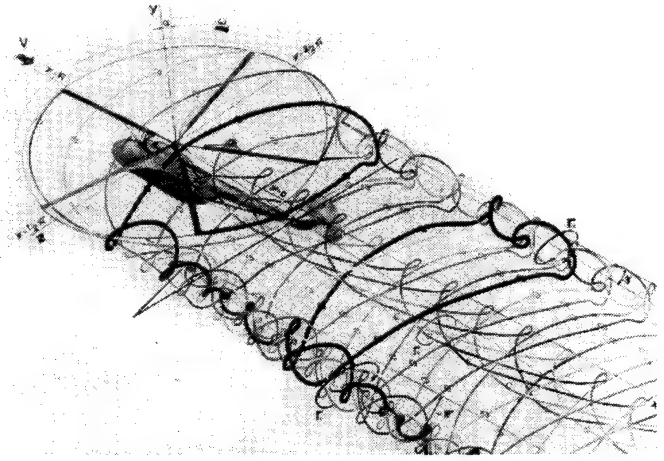

Fig. 2. Vortical wake of a helicopter in forward flight [1].

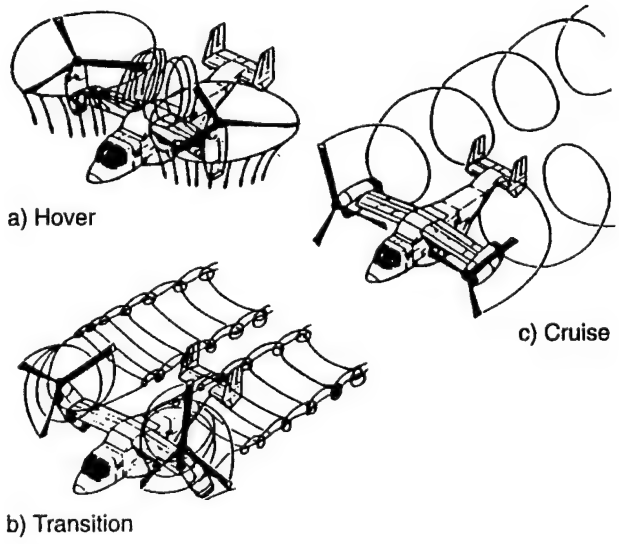

Fig. 3. Vortical flows on tiltrotor aircraft [2].

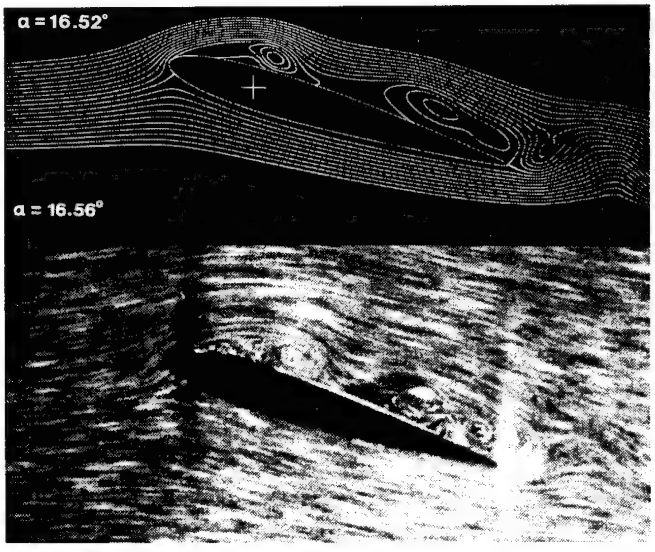

Fig. 4 Calculations [3] and experiment [4] of dynamic stall on an oscillating airfoil.

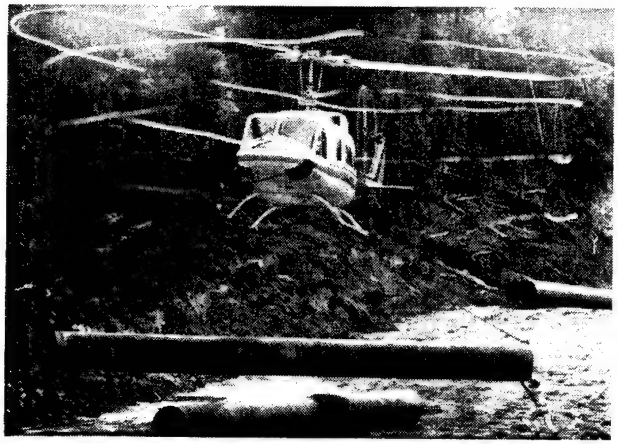

a). visualization by condensation of water vapor in the atmosphere [6]

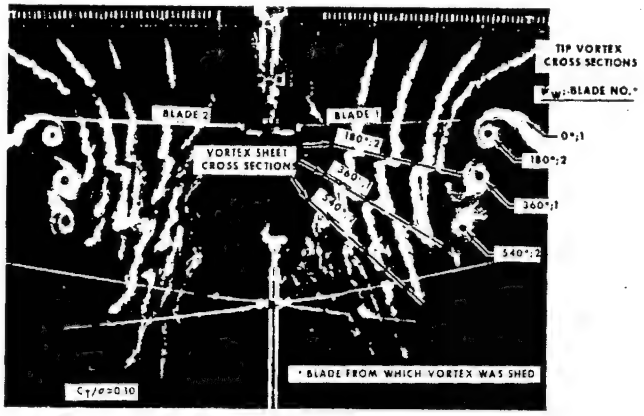

b). smoke injected near the rotor disc [7]

Fig. 5. Tip vortices of helicopter rotors in hover, illustrating tracers introduced in the rotating and nonrotating reference system.

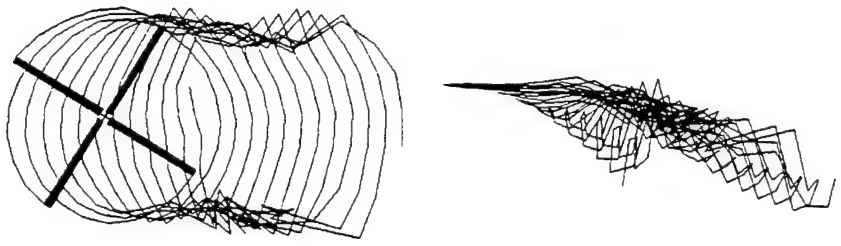

Wake Geometry - FREEWAKE Model, $\mu = 0.1$.

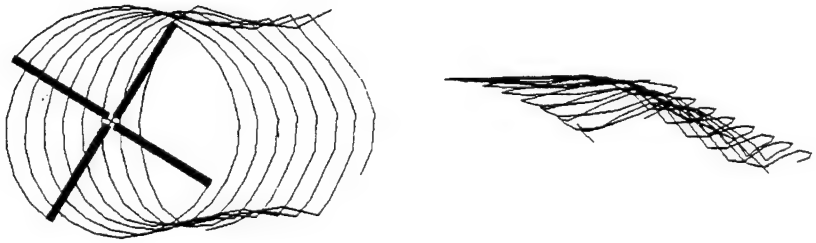

Wake Geometry - Johnson Model, $\mu = 0.1$.

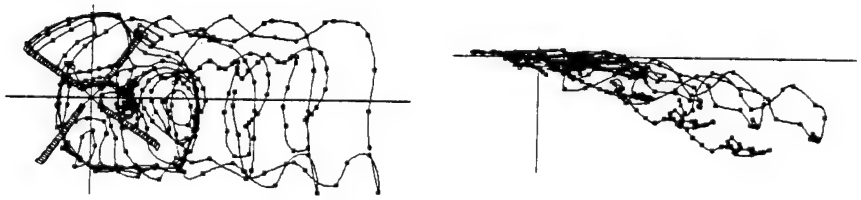

Wake Geometry - rotorCRAFT Model, $\mu = 0.1$.

Fig. 6 Comparison of wake geometry in forward flight predicted by free-wake vortex methods [10-14].

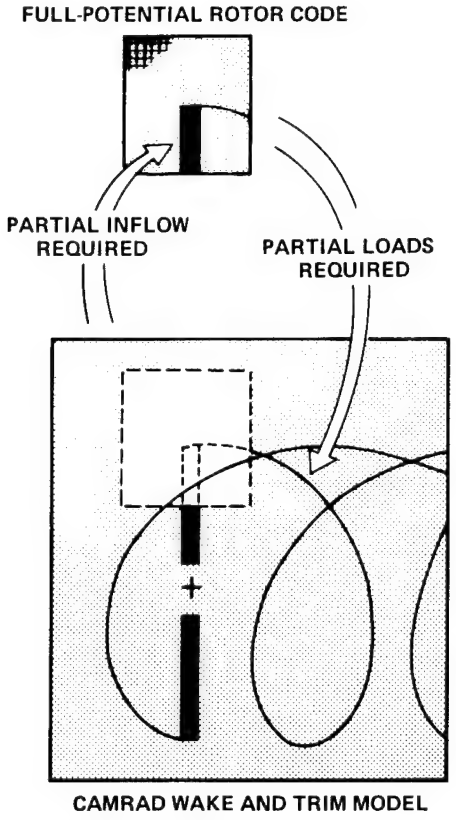

Fig. 7 Scheme for coupling vortex wake methods with CFD aerodynamics codes [16].

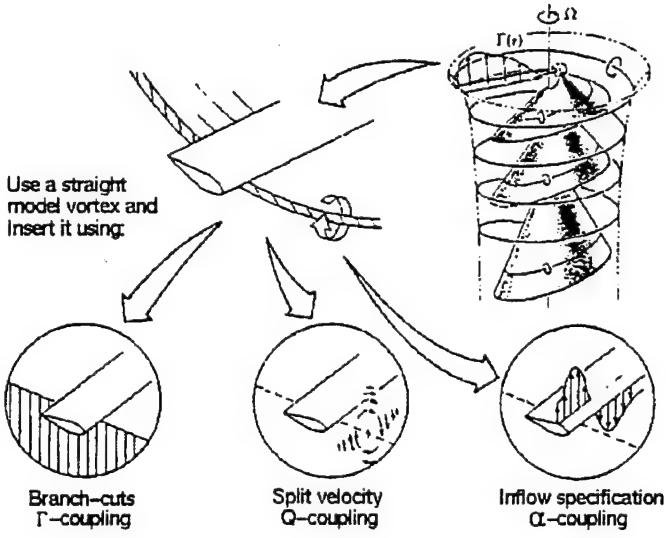

Fig. 8 Near-field blade/vortex modeling methods for use with hybrid methods [6]

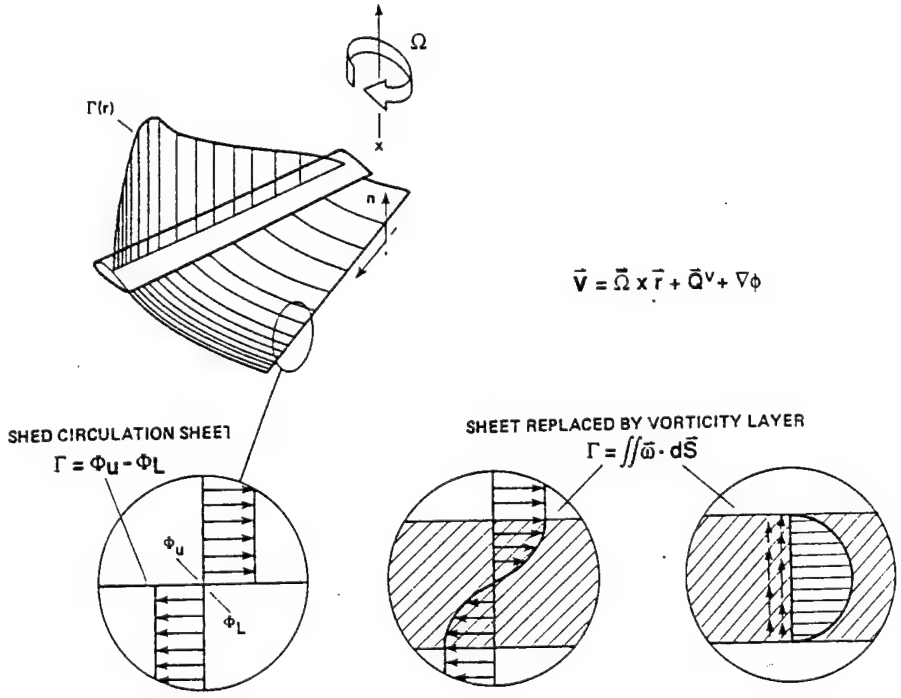

Fig. 9 Alternate models for modeling the shed wake, leading to the "vorticity embedding" method [6,17].

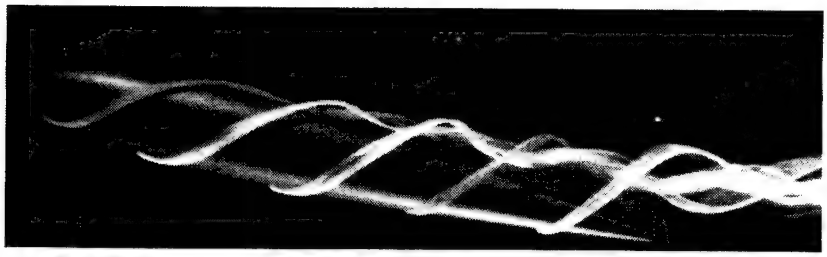

Fig. 10 Tip vortex formation on a wing

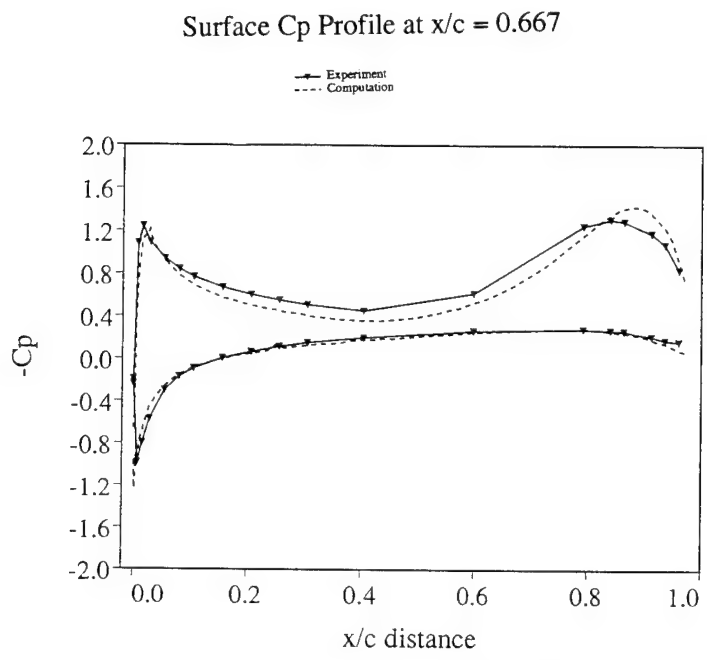

Fig. 11 Calculated and measured pressure distribution near a wing tip

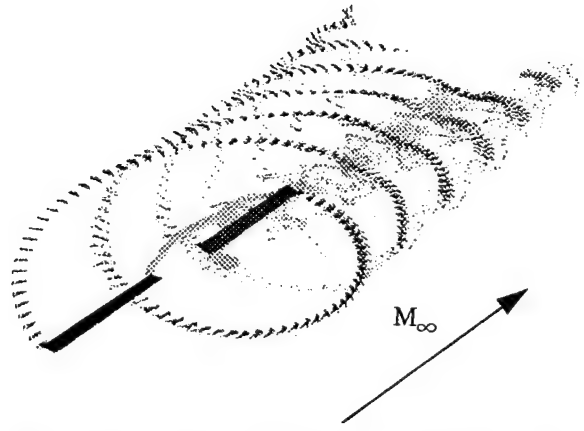

Fig. 12 Computed wake of a rotor in forward flight [28]. Streakline particles released every 5 deg of azimuthal rotation.

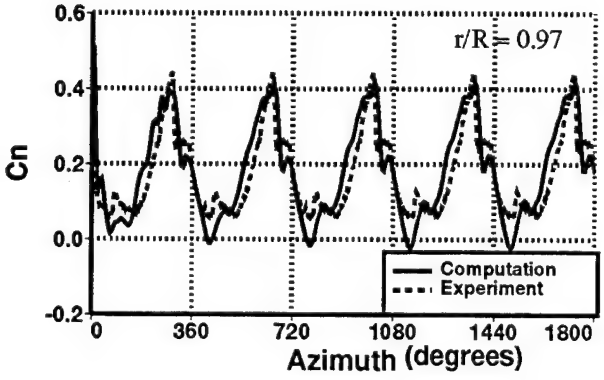

Fig. 13 Time history of blade-element normal force coefficient for the rotor of Fig. 12

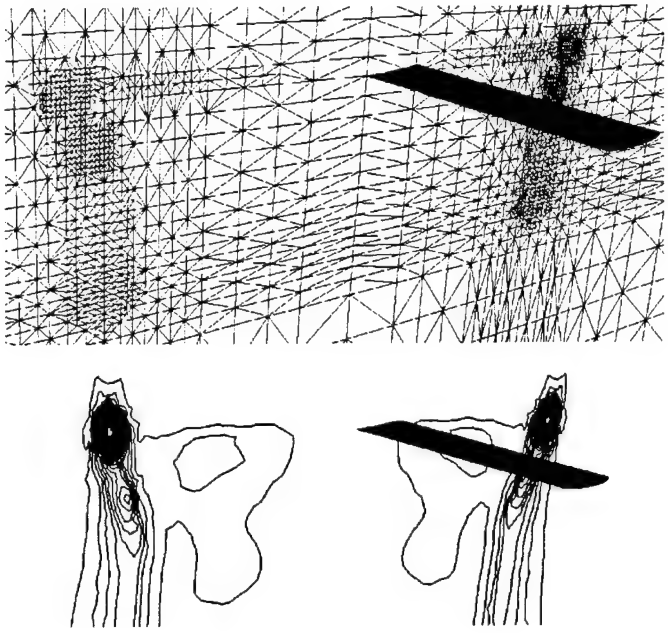

Fig. 14 Solution-adapted unstructured grid and vorticity contours at the boundaries

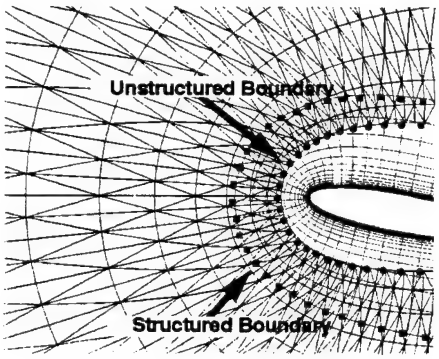

a. overlapping grids near the blade

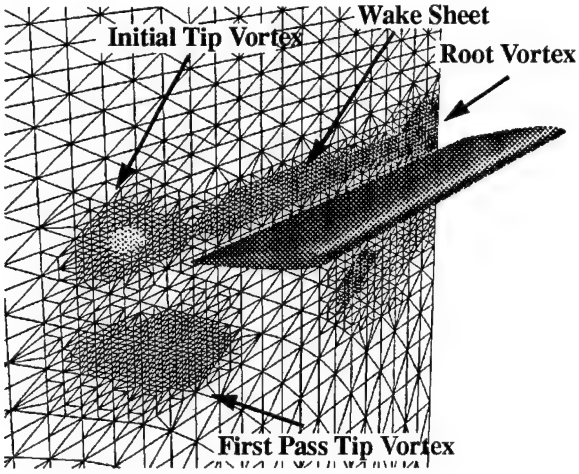

b. solution-adapted unstructured grid

Fig. 15 Hybrid structured/unstructured scheme

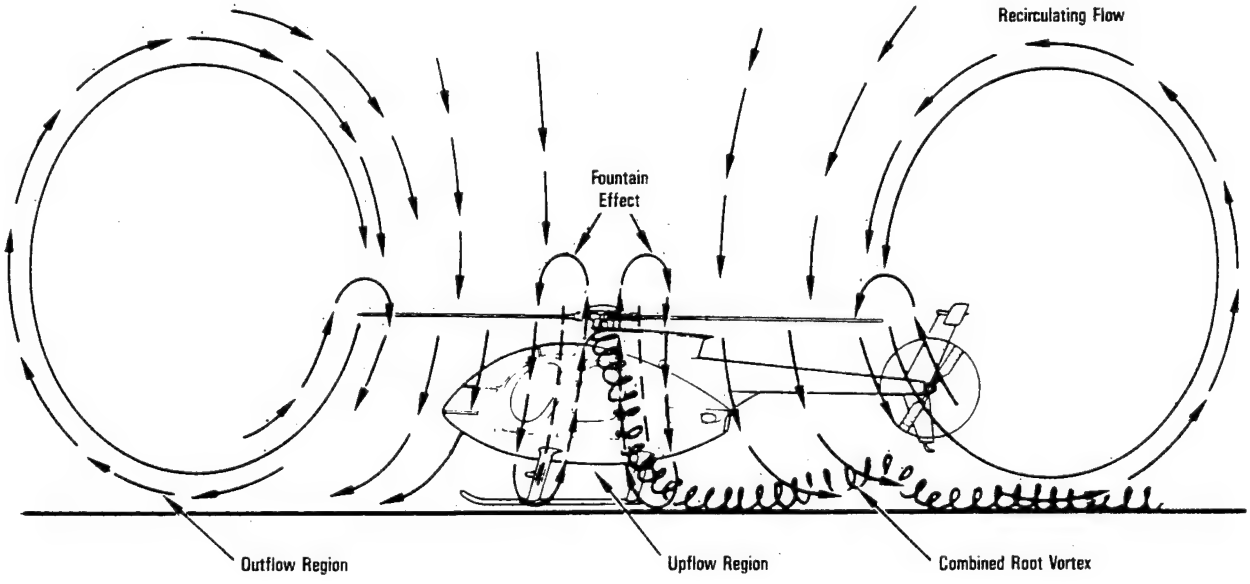

Fig. 16 Flow pattern around a helicopter hovering close to the ground

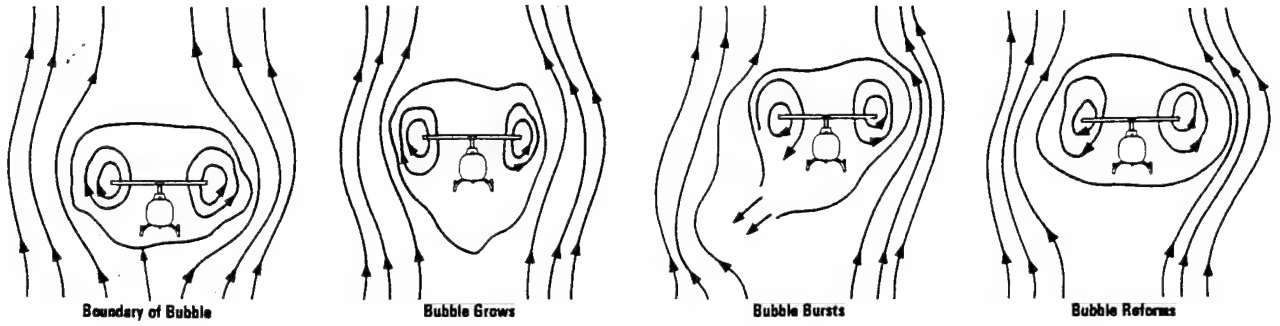

Fig. 17 Vortex-ring conditions for a descending helicopter [36]

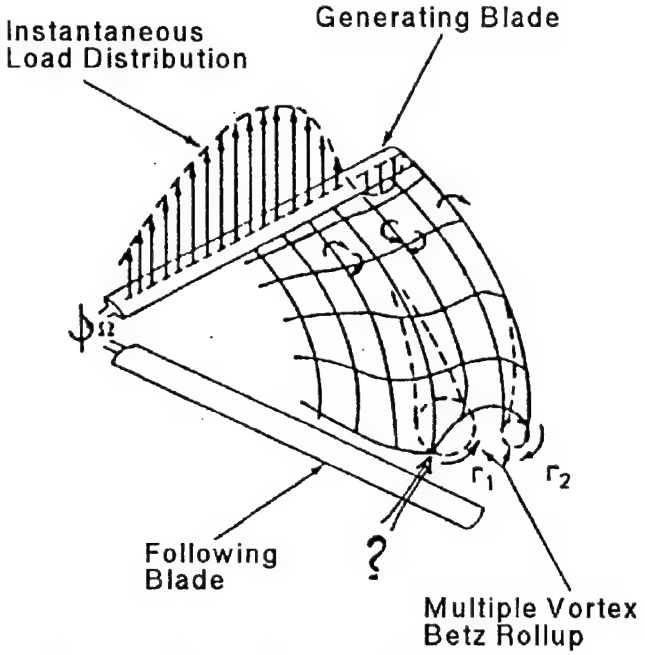

Fig. 18 Schematic of possible wake rollup with multiple vortices

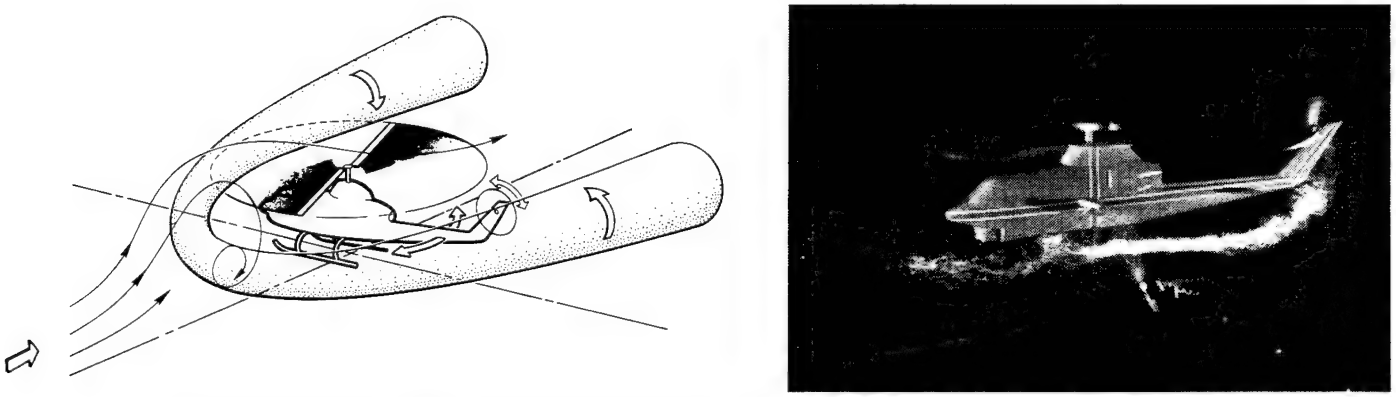

Fig. 19 Main rotor/tail rotor interaction in side wind, with horseshoe ground vortex [47]

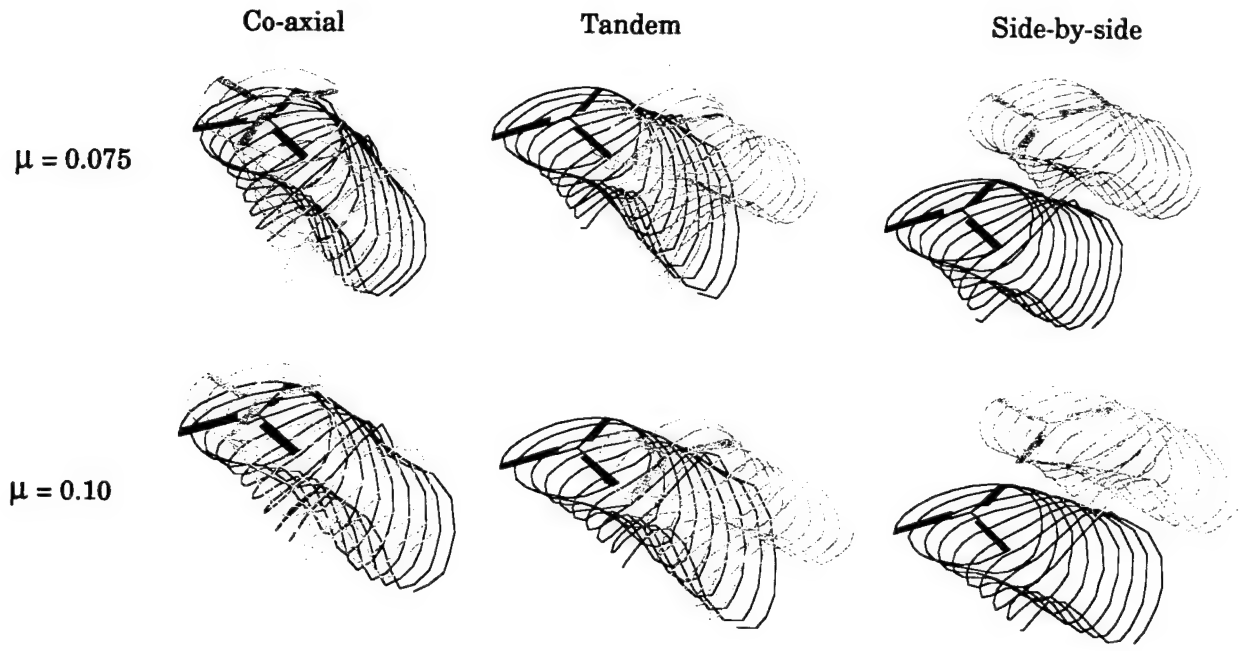

Fig. 20 Isometric views of the computed wakes of three twin-rotor configurations

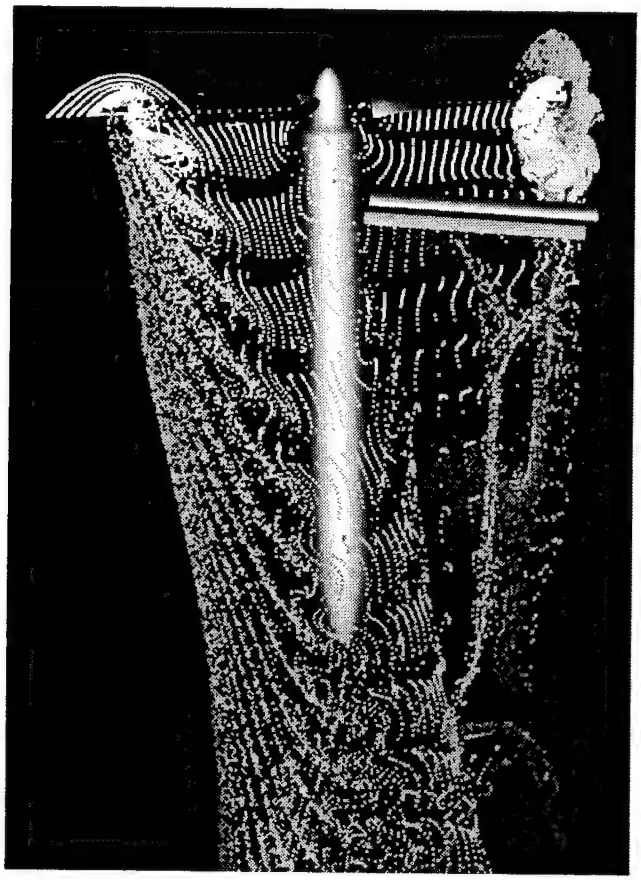

Fig. 21 CFD simulation of rotor/wing interaction in hover, producing the fountain effect

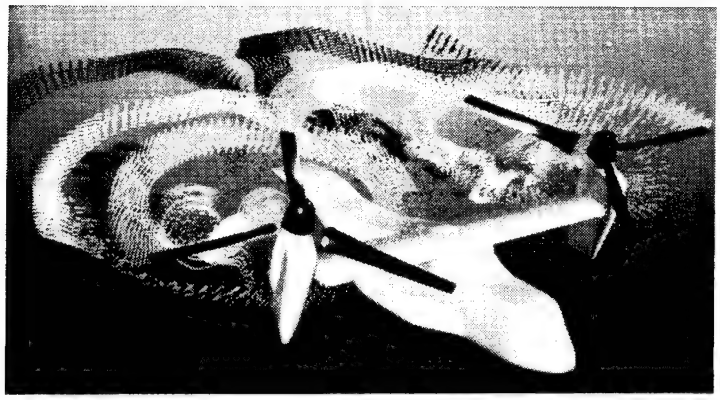

Fig. 22 CFD simulation of the V-22 tiltrotor aircraft at 75 kts. Unsteady particle path traces of the tip vortices

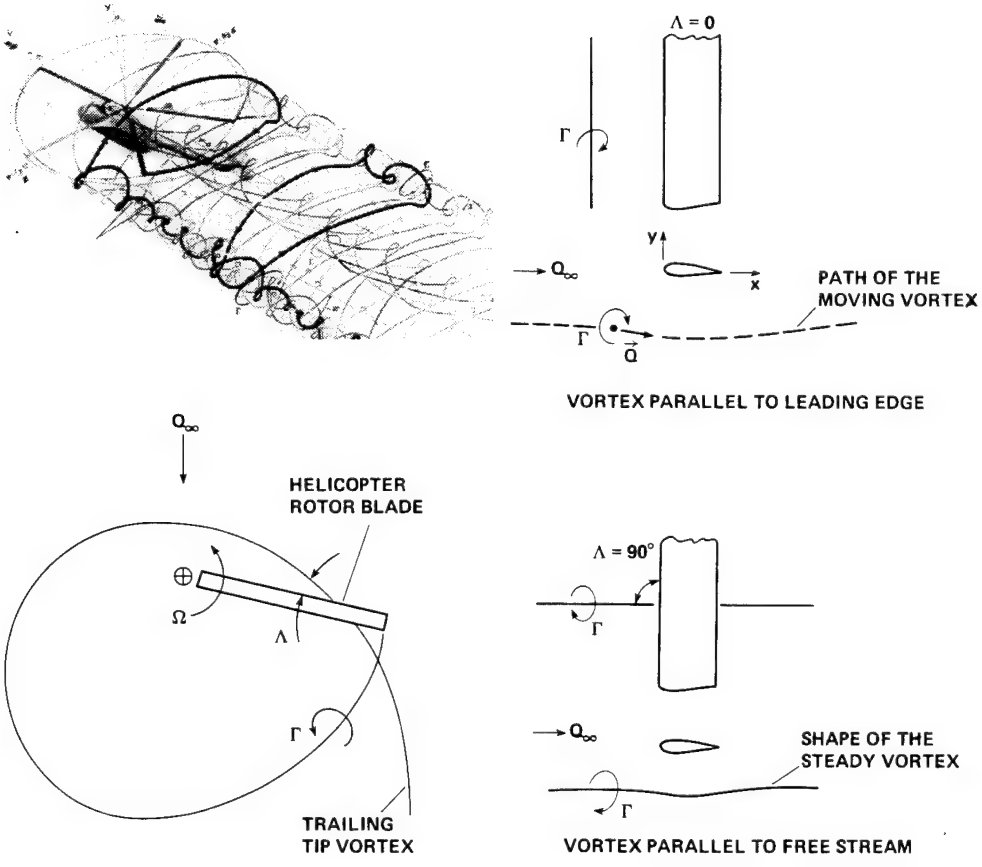

Fig. 23 Blade/vortex interactions of a helicopter rotor in forward flight, including limiting cases for an isolated blade

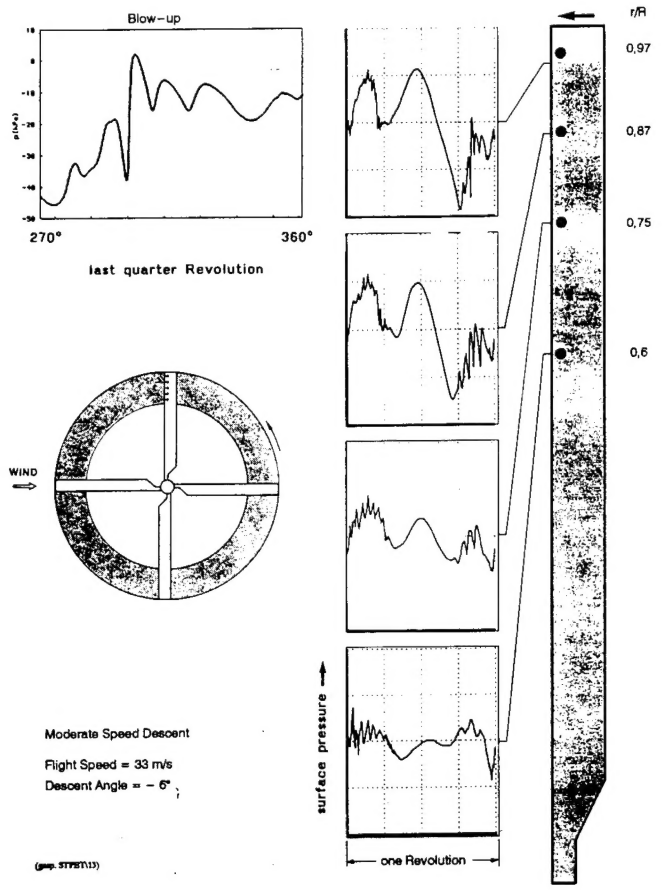

Fig. 24 Time history of upper-surface leading-edge pressure transducers on a rotor during severe blade/vortex interactions

$\mu = 0.149$, $\alpha_S = 5.3°$, $C_T = 0.0045$, $M_H = 0.644$ (6°-DESCENT , 33 m/s)

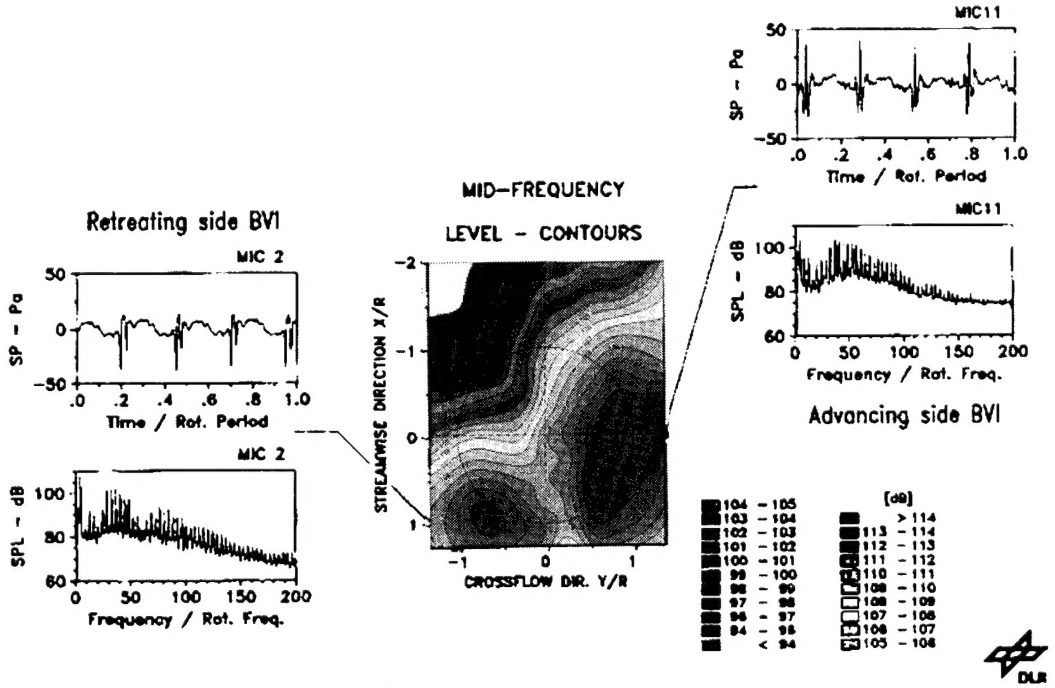

Fig. 25 BVI impulsive noise characteristics for the same conditions as Fig. 24

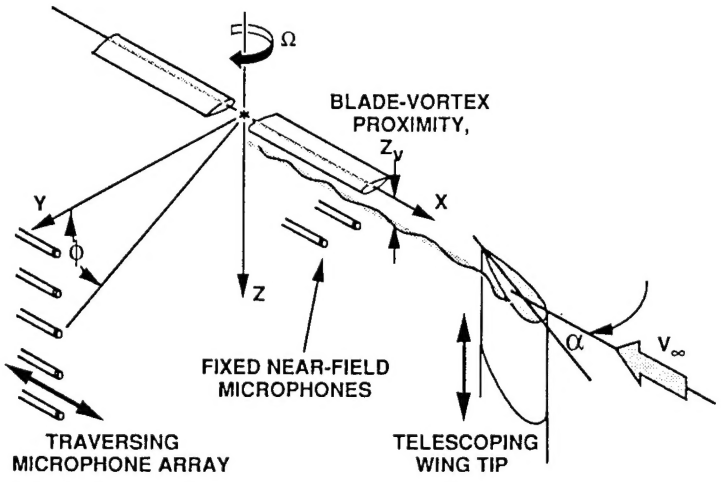

Fig. 26 Special-purpose BVI experimental test configuration, showing wing tip-vortex generator upstream of model rotor

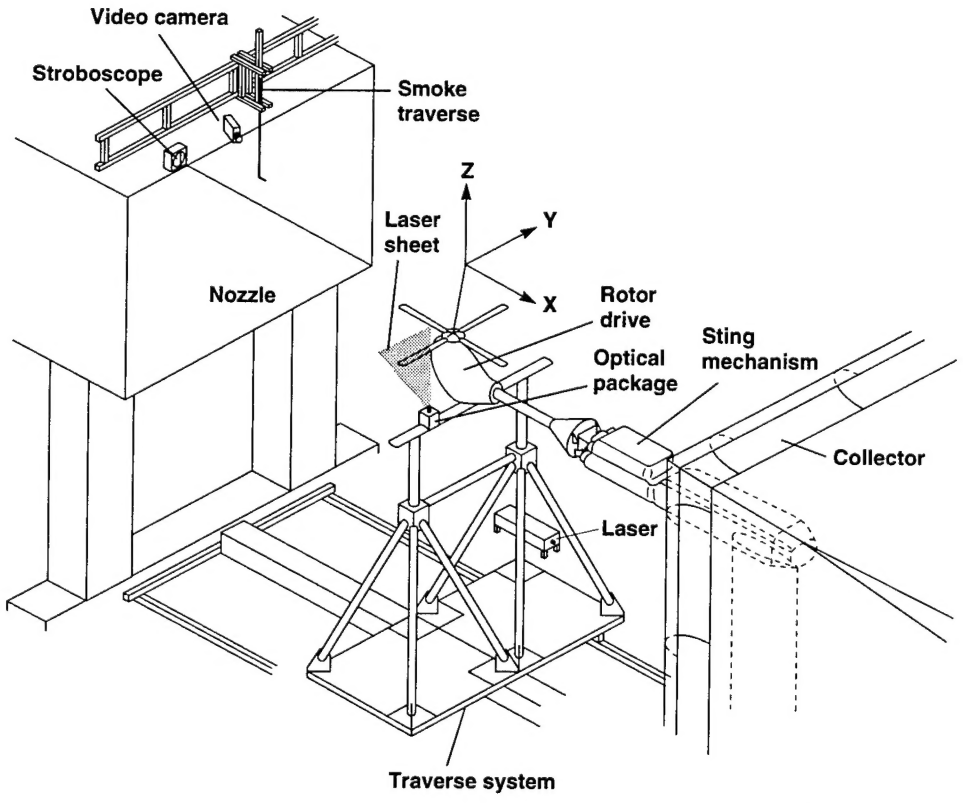

Fig. 27 HART model rotor and instrumentation in the DNW 6m x 8m wind tunnel

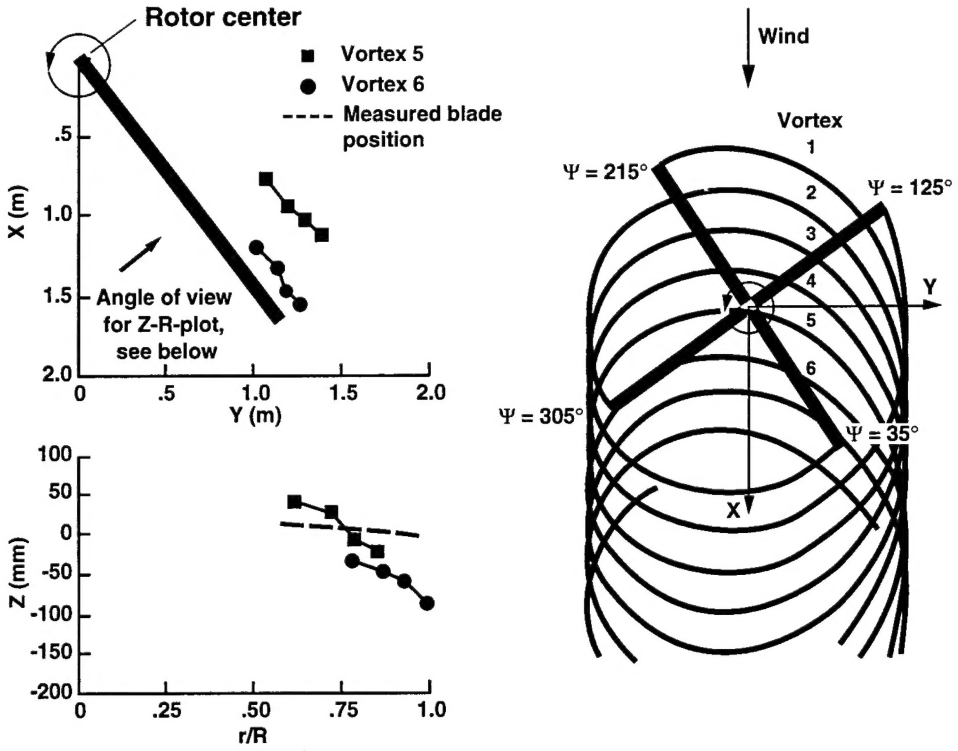

Fig. 28 HART rotor vortex geometry and position relative to the blade

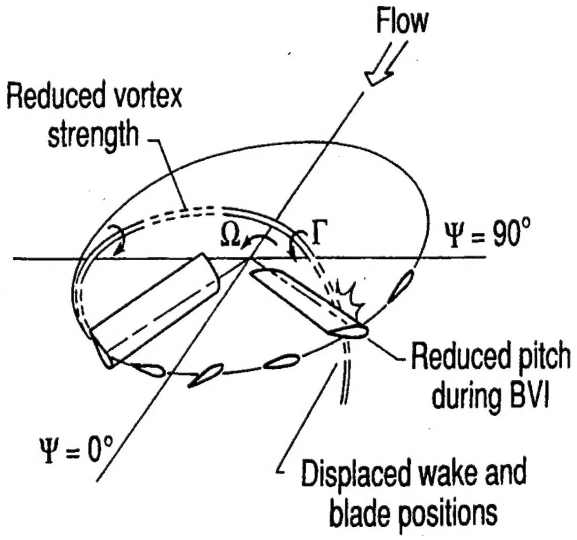

Fig. 29 Sketch of possible mechanisms for BVI noise reduction [67].

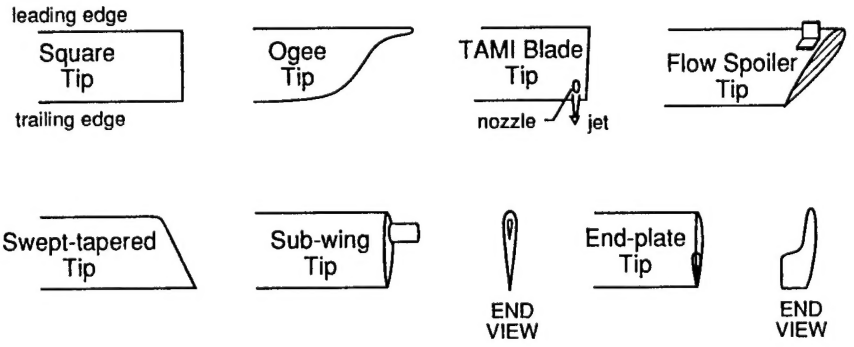

Fig. 30 Some rotor blade tip shapes proposed for BVI noise reduction

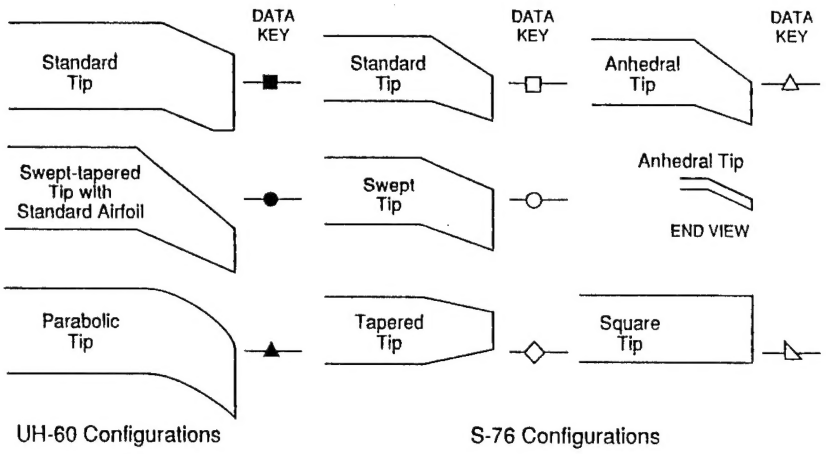

Fig. 31 Some rotor blade tip shapes tested for BVI noise reduction

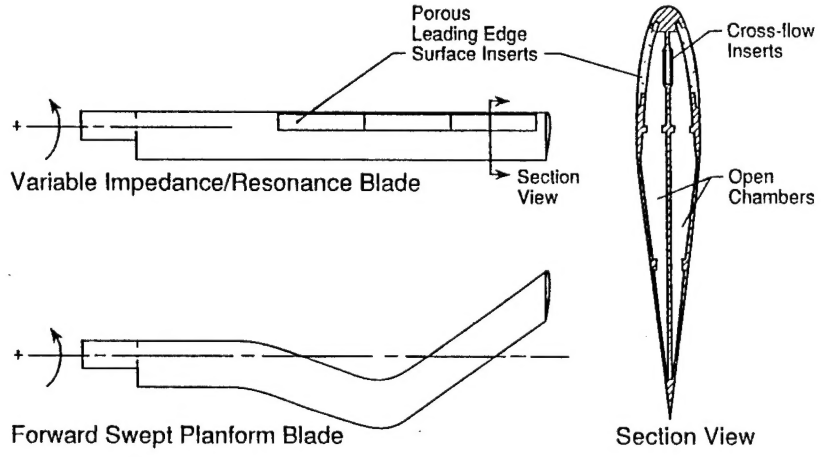

Fig. 32 Additional configurations proposed for BVI noise reduction

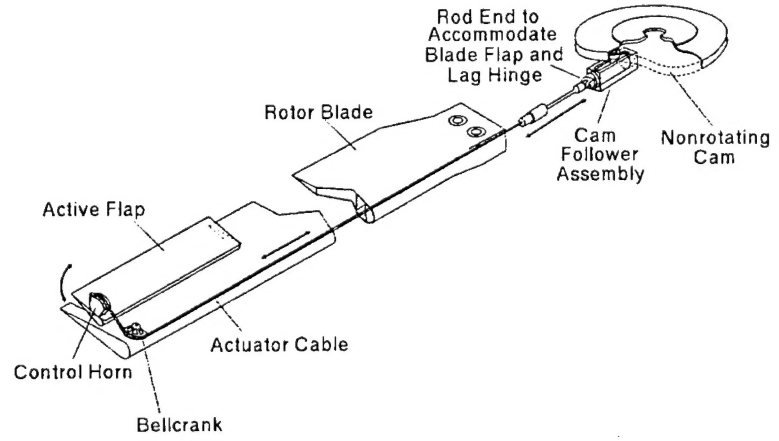

Fig. 33 Rotor blade with active flap tested for possible BVI noise reduction